The Potential Toxicity of Silver Nanoparticles After Repeated Oral Exposure and Underlying Mechanisms in Kidney of Rat Model

Hamed Nosrati
Hamedan University of Medical Sciences
Manijeh Hamzepoor
Hamedan University of Medical Sciences
Maryam Sohrabi
Hamedan University of Medical Sciences
Massoud Saidijam
Hamedan University of Medical Sciences
Mohammad Javad Assari
Hamedan University of Medical Sciences
Nooshin Shabab
Hamedan University of Medical Sciences
Zahra Gholami Mahmoudian
Hamedan University of Medical Sciences
Zohreh Alizadeh (alizadeh.zohreh@gmail.com)
Hamedan University of Medical Sciences

Research Article

Keywords: nephrotoxicity, nanoparticles, apoptosis, growth factor, collagen, kidney

Posted Date: January 4th, 2021

DOI: https://doi.org/10.21203/rs.3.rs-136273/v1

Version of Record: A version of this preprint was published at BMC Nephrology on June 18th, 2021. See the published version at https://doi.org/10.1186/s12882-021-02428-5.

Abstract

Background: Silver nanoparticles (AgNPs) can accumulate in various organs after orally exposure. This study evaluated the toxicity of AgNPs in vivo on histological changes, apoptosis and expression of growth factor genes in kidney.

Methods: The male Wistar rats were treated orally with 30,125,300, and 700 mg/kg silver nanoparticles solution. After 28 days of exposure, histopatological changes were assessed by hematoxylin-eosin, trichrome Masson, and Pas staining. Apoptosis was quantified by TUNEL and immunohistochemistry of caspase-3, and level of expression of growth factors mRNAs were determined using RT-PCR.

Results: Histopathologic examination revealed degenerative changes in the glomeruli, loss of tubular architecture, loss of brush border and interrupted tubular basal laminae. These changes were more noticeable in 30, and 125 mg/kg groups. The collagen intensity was increased in 30 treated groups in both cortex and medulla. Apoptosis was much more evident in middle dose groups (125 and 300 mg/kg). The results of RT-PCR indicated that Bcl-2 and Bax mRNAs upregulated in treated groups ($p<0.05$) and data of the EGF, TNF-α, and TGF-β1 revealed that AgNPs induced more enormous changes in gene expression in 30 and 700 mg/kg groups compared to control.

Conclusion: Our observations showed that the AgNPs played a critical role in their in vivo renal toxicity.

1. Introduction

Advances in nanotechnology have greatly enhanced potential usage in domestic, industrial and biomedical applications. Due to their unique physic-chemical, and biological properties, silver nanoparticles are the most widely used among metal nanoparticles, which is confirmed by a significant increase in the number of products that contain AgNPs from about 30 in 2006 to more than 435 in 2015(1, 2). Because of their small sizes, the AgNPs can enter the human body through ingestion(3), inhalation(4), and also skin contact(5). Kidneys, lungs, nervous system and liver are potent organs for the accumulation of AgNPs, depending on the concentration and size (4, 6). Induction of inflammatory and cytotoxicity effects of AgNPs in different cells and tissues have been reported through in vitro and in vivo studies (6-8).

Metal nanoparticle toxicity induction mechanisms are attributed to the reactive oxygen species (ROS) generation and the release of cytokines, which leads to cell changes, including DNA damage and apoptosis(9).

Decreased renal function due to apoptosis of intrinsic renal cell populations is a characteristic feature of renal disorders caused by different etiologies, such as toxins. Enhanced apoptosis has been shown to lead to glomerulosclerosis and tubular atrophy, as well as interstitial scarring.

The induction or suppression of apoptosis is affected by many growth factors. Epidermal Growth Factor (EGF) has an in vitro protective effect on renal cells from apoptotic stimuli such as serum deprivation (10). In contrast, it has been reported that transforming growth factor β1 (TGF-β1) and Tumour Necrosis Factor α (TNF-α) induce apoptosis in renal fibroblasts, tubular epithelial cells (11, 12), and glomerular epithelial cells (13).

In the present study, we investigate the histological alterations, apoptosis, and correlations of altered expression of genes influencing apoptosis in the renal tissue in rats exposed to AgNPs at doses of 30, 125, 300, and 700 mg/kg for 28 days.

2. Material And Methods

2.1 Animals

In a controlled environment of the animal house (21±2°C temperature, 50±15% humidity and a 12-h light/dark cycle), forty 10-12 week old adult male Wistar rats (180-200 g) were housed during the experimental period (28 days) and allowed free access to water and food. The animal body weights were recorded before and after AgNPs treatment. The body weight gain was calculated from the final body weight minus initial body weight. Renosomatic index (RSI) was calculated according to the following standard formula: RSI = Kidney weight (g)/body weight (g) × 100

2.2 Silver nanoparticles

The suspension of AgNPs powder (CAS No. 7440-22-4) was performed in accordance with the procedure described in our previous study(14). Briefly, Different concentrations of AgNPs (30, 125, 300, and 700 mg) were dispersed in deionized water by vortexing and followed by sonication for 10 minutes. The distribution of particle-size of the AgNPs was measured using dynamic light-scattering (DLS) technique by Malvern Zetasizer (Nano ZS ZEN- 3600, UK). Transmission electron microscope (TEM) (Philips-EM 208) was used to determine the size and shape of the nanoparticles.

2.3 Experimental design

Animals were randomly divided into four treatment groups and a control group (n=8 for each group). Rats in the first four groups were administered 30, 125, 300, and 700 mg/kg of AgNPs suspension orally for 28 days. Equal volumes of deionized water were administered orally to the control group. Animals were sacrificed 24 h after the last administration to harvest and weigh their kidneys. One kidney of each rat was frozen in −80 °C for molecular studies, and the other kidney was immersed 10% neutral buffered formalin solution for further histopathological investigations.

2.4 Histological Study

The fixed tissues using the standard technique were processed routinely, embedded in paraffin, and 5 µm-thick sections were prepared for hematoxylin and eosin (H&E) staining. Special staining techniques, Masson's trichrome, and periodic acid Schiff (PAS) were done to evaluate the collagen deposition changes and also brush border and tubular basal lamina, respectively. All the images were acquired by a motic 2000 camera (Kowloon, Hong Kong) attached to a Nikon Eclipse E800 research transmitted light microscope (Melville, New York, USA). The motic images 2.0 software were used for H&E and PAS stained sections and image J for Masson's trichrome stained slides to the acquisition of the variations in histomorphology of groups.

2.5 TUNEL (terminal deoxynucleotidyl-mediated dUTP nick labeling) assay

A TUNEL assay kit (Promega, Co., Madison, WI) was used to assess cell apoptosis in the renal tissues, as instructed by the manufacturer. Paraffin-embedded tissue sections were deparaffinized, rehydrated, and permeabilized with proteinase K solution for 30 minutes. Tissue sections were then incubated with biotinylated nucleotide mix, recombinant terminal deoxynu-cleotidyl transferase, and equilibration buffer for 1 h at 37 ∘C. The sections were incubated in a converter-POD solution for 30 min after rinsing with PBS. Dehydration was performed using graded ethanol. Sections were covered with mounting medium (Scytek Laboratories, Logan, UT, USA) and counterstained with hematoxylin Mayer. During the tailing reactions, TdT was eliminated as a negative staining control.

The average number of apoptotic cells was determined by counting TUNEL positive cells in five neighboring medium-power fields and dividing the total by five and expressed as percentage.

2.6 Immunohistochemistry

Changes in the distribution and expression of the caspase-3 protein in the renal tissues were evaluated by immunohistochemistry in prepared kidney sections. Briefly, tissue sections of 4-µm thickness were sequentially deparaffinized, rehydrated, and submitted to antigen retrieval. The sections were incubated overnight at 4 °C with the rabbit anti caspase-3 antibody (ab13847, 1:200) diluted in PBS. After washing the secondary antibody bond to the biotin (Detection Kit Goat Anti-Rabbit HRP (IgG) (Ab6721) Abcam) was applied for 15minuts, and then the Avidin, HRP conjugate was added and incubated in a moisture box at room temperature for 15 min. The results were developed using DAB, and sections were mounted and observed under a microscope. Immuno-positive cells were counted and expressed in ‰.

2.7 Blood Biochemistry

Blood samples were collected by cardiac puncture and allowed clotting for 45 minutes at room temperature. The serum was separated by centrifugation at 1500 g for 10 minutes. Blood urea nitrogen (BUN)and creatinine were measured using an autoanalyzer (Hitachi 7180, Hitachi, Japan) and biochemical kit.

2.8 RNA extraction and quantitative real-time polymerase chain reaction

Total RNA was extracted from the renal tissues of rats by TRIzol® reagent (Invitrogen), according to the protocol provided by the manufacturer. The RNA concentration was determined using an Epoch Microplate Spectrophotometer (Biotek, USA). Extracted RNA was reverse transcribed into single-strand cDNA using RevertAid™ first-strand cDNA synthesis kit (Thermo Scientific) according to the manufacturer's instructions. The transcription process included incubation of the reaction mixture at 20°C for 30 s, followed by 5 min at 44°C, 30 s at 55°C, and 5 min at 95°C. The cDNA was stored at -80°C until further use for PCR.

Quantitative real-time PCR analyses were carried out using the SYBR premix Ex Taq 2 kit (Takara) in a final volume of 25 µl with 10 pmol of each primer by CFX96 real-time PCR detection system (BioRad, USA). Each assay was run in the triplicate manner with each set of primers. The sequences of primers, accession number, and primer-specific annealing temperature have been presented in Table 1.

Table 1. Primers features of the studied genes

Gene	accession number	Primer sequence	annealing temperature
Bax	NM_017059	F: GAGACACCTGAGCTGACCTTG R:CCTGCCACACGGAAGAAGACCTC	55
Bcl-2	NM_016993	F: CGGGAGAACAGGGTATGATA R: TCAGGCTGGAAGGAGAAGATGC	54
EGF	NM_012842	F: AACTGTGTCATTCCAGGATC R:CGAGTCCTGTAGGATCGCCAT	55
TGF-β1	NM_021578.2	F: ATTCAAGTCAACTGTGGAGCAAC R: CGAAAGCCCTGTATTCCGTCT	57
TNF-α	NM_012675.3	F: TGTTCATCCGTTCTCTACCCA R: CACTACTTCAGCGTCTCGT	55
18SrRna	NM_031144	F:CGGAAGACTCACACCTTGA R:GTCCTCAGTGTAGCCCAAGA	53

Cycle threshold (Ct) values were achieved through the auto Ct function. The mean CT value was determined after efficiency correction and then normalized to the reference gene (18S rRNA) using delta (Δ)CT. The relative expression changes were determined using the $2^{-\Delta\Delta ct}$ method(15).

2.9 Statistical analysis

Statistical analysis was performed using the SPSS 16.0 software (SPSS Inc., USA), and the data are presented as mean ± standard deviation (SD). The significant statistically changes were determined using a one-way analysis of variance (one-way ANOVA) and Tukey test. P-values less than 0.05 ($p<0.05$) were considered statistically significant changes. Pearson's correlation analysis was employed to determine the correlation values (r) between parameters.

Ethical statement: The above-mentioned treatment/sampling protocols were approved by the ethics committee of Hamadan University of Medical Sciences (ethical code: IR.UMSHA.REC.1394.553) and all methods were carried out in accordance with the relevant guidelines and regulations. The study was carried out in compliance with the ARRIVE guidelines.

3. Results

3.1 Nanoparticles characterization in solution

The AgNPs suspension was subjected to dynamic light scattering (DLS) analysis to determine the diameter of the silver nanoparticles. It exhibited a hydrodynamic diameter peak, with an average size of 200-300nm. The TEM images of AgNPs showed that the majority of AgNPs were spherically shaped with smooth surfaces (data not shown).

3.2 Body and organ weight

Table 2 shows the results of body weight gain and the renosomatic index. There were no significant dose-related changes in the body weight gains of rats. No significant renosomatic index was observed in treated rats except for an increase ($P < 0.05$) in the index of the right kidney for the 30 mg/kg dose rats.

3.3 Effects on Clinical Chemistry

In this study, kidney function was evaluated with serum levels of BUN and creatinine. These parameters showed no statistically significant difference between experimental and control groups after 28 days of exposure to AgNps (Table 2).

Table 2 .Body weight gain and renosomatic index and serum values of BUN and Creatinine after 28-day oral administration of silver nanoparticles (mean ± S.D.)

Groups	Body weight gain	Leftrenosomatic index	Rightrenosomatic index	BUN(mg/dL)	Creatinine(mg/dl)
Control	72.72±19.50	0.37±0.05	0.35±.04	67.60 ±4.72	0.70 ±0.07
30 mg/kg	61.02±8.045	0.42±0.02	0.43±0.04*	62.25 ±3.20	0.70 ±0.08
125 mg/kg	76.63±18.57	0.37±0.03	0.36±0.04	59.50 ±1.73	0.68 ±0.05
300 mg/kg	64.52±7.98	0.35±0.03	0.36±0.02	62.50 ±5.00	0.78 ±0.05
700 mg/kg	67.05±2.29	0.36±0.03	0.37±0.02	62.50 ±3.00	0.60 ±0.08

*Significant difference vs. control, $p < 0.05$

3.4 Histological evaluation

3.4.1 H&E-stained sections

Renal sections from the control group showed typical histological structure in different parts such as renal corpuscles, proximal and distal convoluted tubules, and also the interstitial tissue. Sections from AgNPs treated groups showed many forms of glomerular, tubular, and interstitial affections (Fig1).

Glomerular alterations: The cortex showed partial destruction of renal corpuscles with collapsed glomerular tufts, widening of Bowman's space, and necrosis (Fig 1). The mean glomerular diameter was also measured. This parameter reduced significantly in the treated group of 125mg/kg compared to the controls ($p<0.05$).

Tubular alterations: In AgNPs treated groups, loss of tubular architecture was seen, and the epithelial lining of the tubules in cortex showed cytoplasmic necrosis and vacuolation. Luminar site of several cortical tubules displayed dense acidophilic hyaline casts. Also, shedding and desquamation of the lining epithelium were observed more prominently in proximal tubules of 30, and 125 mg/kg treated groups (Fig 1).

Interstitial tissue alterations: The most significant histological changes in renal interstitial tissue including, infiltration of inflammatory cells and congestion, were observed in rats exposed to 125, 300, and 700 mg/kg of AgNPs (Fig 1).

	control	30mg/kg	125mg/kg	300mg/kg	700mg/kg
Mean glomerulus diameter (µm) ±SD	237.5±67.65 c	180.73±27.95	152.78±49.58 ade	213.73±70.15^{c}	236.32±68.85^{c}

3.4.2 PAS-stained sections

In relation to PAS staining, disruption of brush border and basement membrane integrity were observed in 30 and 125 mg/kg AgNPs-treated groups in the renal tubules in comparison with the control group. The cortical tubules from 300 and 700 mg/kg showed a protected brush border and also continuous basal lamina (Fig 2).

3.4.3 Masson's trichrome-stained sections

Masson's trichrome quantified the intensity of blue (representing Collagen deposition) within renal tissue. The blue intensity was increased in 30($p<0.05$) and 125($p>0.05$) mg/kg treated groups in both cortex and medulla. The 300 and 700 mg/kg treated groups, indicated that Collagen content is almost similar in normal renal tissues (Fig 2). PAS staining confirmed Masson's trichrome staining results for collagen sedimentation.

3.5 TUNEL assay

To assess the effect of AgNPs treatment on renal tubular cell apoptosis, renal tissue sections were examined by performing terminal deoxynucleotidyl transferase–mediated digoxigenin-deoxyuridine nick-end labeling TUNEL staining. As illustrated in Figure 3, the number of TUNEL-positive tubular cells was increased in 125($p>0.05$) and 300 ($P<0.05$) AgNPs groups compare to control, 30, and 700 mg/kg AgNPs treated groups.

3.6 Immunohistochemistry

The percentages of caspase-3 positive cells were obtained in the stained slides. The results are shown in Fig 3, which shows a significant difference in the expression of caspase-3 in the groups of 125, 300, and 700 mg/kg compared to the control group ($P < 0.05$).

3.7 Expression of genes influencing apoptosis

As illustrated in Figure 4, Bax mRNA concentration was increased in 30 and 700 mg/kg treated as compared to the controls group. However, the expression of this gene increased in 125 and 300 mg/kg treated groups, but this increase is not statistically significant ($P<0.05$). The expression of Bax in groups of 30, 125, 300, and 700 mg/kg was 4.47, 1.91, 1.69, and 3.96 times, respectively, compared to the control group.

Bcl-2 mRNA concentration was increased significantly in 30, 300, and 700 mg/kg treated as compared to the controls group ($P<0.05$, Figure 4). The average amount of Bcl-2 gene expression in groups of 30, 125, 300, and 700 mg/kg was increased by 6.37, 2.16, 4.42, and 11.69 folds, respectively.

The Bax /Bcl-2 ratios of the mRNA levels are shown in Fig 4. The ratios were significantly increased in 300, and 700 mg/kg treated groups compared to control.

3.8 Growth factor gene expression

Analysis of the expression of growth factors revealed the upregulation of the EGF mRNA concentration in 30, 125, and 700 mg/kg treated groups as compared to control (Fig 5). TNF-α mRNA expression was also increased in 30, 125, 300, and 700 mg/kg. Data from TGF-β1mRNA expression showed no statistically significant difference between the control group and experimental groups despite the increased expression of this gene was seen in groups of 30 and 700 mg/kg ($P>0.05$).

3.9 Correlation between apoptosis and the expression of genes influencing cell death

A significant positive correlation was observed between the mRNA levels of Bax and Bcl-2 (r=0.850; P=0.0001). The caspase-3 expression was correlated with ratio of ΔctBax /ΔctBcl-2 (r=0.477, p = 0.03) and TUNEL+ cells (r = 0.547, p = 0.01). The correlations between TGF-β1, TNF-α and EGF mRNA expression and transcription levels of Bax and bcl2 are shown in table 3.

Table 3. The correlation between apoptotic related genes and expression of growth factors in 28 orally AgNPs treated rats

Δct Bcl-2	**Δct** Bax	
r=0.636(p=.003)	r= 0.802(p=0.001)	**Δct TGF-β1**
r=0.749(p=.001)	r=0 .610(p=0.006)	**Δct TNF-α**
r=0.674(p=0.002)	r=0.895(p=0.001)	**Δct EGF**

4. Discussion

The toxicity of AgNPs has been considered as an important part of nanotoxicology(16). Exposure to AgNPs can occur in different ways, including dermal contact, inhalation, and ingestion (17, 18). Oral route as a kind of exposure route of AgNPs, may be important in many industries, food, and medicine products.

AgNPs exposure leads to particles translocated to the blood and distributed throughout various organs, particularly the kidneys, liver, spleen, brain, and lungs (19). Kidneys are known as one of the most vulnerable organs after prolonged exposure to nanoparticles (6). Kim et al. showed that AgNPs accumulated in the kidney after oral administration for 28 to 90 days(6). Plus, the deposition of nanoparticles and silver can occur along the mesangium and glomerular basement membrane(20, 21). That is why the present study was conducted to study the adverse effects of silver nanoparticles on rat kidney treated with repeated oral administration for 28 days by examining the body weight, renosomatic index, histology, apoptosis, fibrosis, and expression of some growth factor genes in kidneys.

There were no significant dose-related changes in the body weight gains of rats. No significant renosomatic index was observed in treated rats. These results agreed with Kim(6) and Ji(4) that did not show any significant changes in body weight and renal index relative to various concentrations of AgNPs during the 28-day experiment by oral and inhalation exposures.

BUN and creatinine were not increased significantly compared to control, but inflammatory responses were observed in the kidney. It seemed that the inflammatory responses are too week to impair the filtration capacity of the kidney. Other studies using different doses and duration also showed the same results (6, 19, 22).

Histopathological examination of kidney show dose-dependent AgNPs induced lesions in renal corpuscles, tubules, interstitial tissues, and inflammation. Partial to complete damage to the number of renal corpuscles with loss of glomerular capillary tufts were observed. The morphometry studies confirmed this by revealing a significant decrease in the diameter of affected renal corpuscles compared to the control. However, these changes are more prominent in 30, and 125 mg/kg treated groups. Marked glomerular capillary-tuft distortion or complete loss was described in case of severe renal injury and toxic conditions (23-25).

The results of histology of lining tubular epithelial cells showed damage, including vacuolization, cloudy swelling, severe necrosis, pyknotic nuclei, and degenerative changes together with desquamation of degenerated cells and shedding in the lumen of the tubules. Complete or partial loss of brush border, interrupted basal laminae, and tubular dilatation with intraluminal dense acidophilic hyaline casts were also evident. The results of this study showed that these changes were more frequent in the 30 and 125 mg/kg groups, indicating toxicity induction by these doses. In confirmation of the effect of toxic substances on vacuolar degeneration and cloudy swelling, the results of the effect of cisplatin and different kinds of nanoparticles showed the same results (26-28). Almost all observed cytoplasmic and nuclear degenerative changes in proximal tubules were more evident than distal tubules. This could be because the main and primary site of reabsorption and active transmission is proximal tubules(29).

The hyaline casts represent injured tubular epithelium. The hyaline casts form cellular debris that have undergone molecular changes. Cells and their debris, which are detached from the tubular basement membrane, interact with proteins in the tubular lumen, leading to cast formation. In addition, impaired sodium reabsorption, due to the damaged tubular epithelium results in increased sodium concentration in the lumen of tubules causing protein polymerization and contributing to cast formation (30).

Regarding vascular alterations, consistent with our results, other studies reported that different nanoparticles with different sizes and duration resulted in expanded and congested renal tubular capillaries with inflammatory infiltration(22, 25). It has been reported that cell infiltration is a sign of atrophy of tubular cells in chronic kidney disease(31). This inflammatory response seems to be a result of the oxidative stress caused by AgNPs and contributing to vascular congestion.

Interstitial tissue fibrosis involves excessive accumulation of collagen fibrils and is a common feature of many diseases that progress to chronic renal failure(32). Results of this study revealed marked deposition of collagen within the glomeruli and also between renal tubules in the 30 and 125 mg/kg treated groups than in other groups. In the formation of renal interstitial fibrosis, a variety of inflammatory cells and growth factors such as TGF-β1 participate. TGF-β1 is regarded as a key mediator of renal interstitial fibrosis(33). In our study, expression of TGF-β1 was increased in 30 and 125 mg/kg AgNPs treated groups almost 3.98 and 3 fold of the control group, respectively. Also, the mean area percent of collagen fibers in 30 mg/kg group was significantly higher than the control.

In the present study, it seems that obtained more severe histological changes in rats administrated 30 and 125 and slight damage in 300 and 700 mg/kg/day be due to translocation of AgNPs into the kidney.

It may be due to the agglomeration of AgNPs used in this study (~250 nm hydrodynamic diameter agglomerates). The small intestine is the first site for nanoparticles to be absorbed following oral administration. Agglomeration of AgNPs in high concentrations may also have hindered their intestinal absorption and so resulted in an insufficient amount of AgNPs being available to the kidney. Kim et al. reported similar results(6).

The number of renal cells during the development and progression of renal disorders is regulated by apoptosis(34). Through studying the gene expression of apoptotic regulatory and effector molecules in different doses of AgNPs treated rats, we obtained a greater understanding of the control of apoptosis in the affected kidney.

Bcl-2 is an apoptosis inhibitory factor, while Bax promotes the process of apoptosis in various tissues. The state of cell apoptosis is determined by the ratio of their level of expression(35). We examined whether the increased ratio of these genes is related to the process of apoptosis in the renal tissue of the AgNPs treated rats. It was found that the number of caspase-3 positive cells were significantly increased in rats treated with 125 and 300 mg/kg within interstitial and tubular epithelial cells. Furthermore, the ratio of Bax /Bcl-2 mRNA was correlated with caspase-3 positive cells. The findings indicate a possible implication of Bax and Bcl-2 in the apoptotic process during AgNPs treatment.

TUNEL, caspase-3, and Bax /Bcl-2 mRNA evaluation showed a lower rate of apoptosis in 30 mg/kg group compare to other tested groups. Given the lack of association between apoptosis (caspase+cells) and fibrosis or glomerular and tubal injury, the alternative non-apoptotic pathways may be activated in this group as more prominent necrosis were found more in 30 mg/kg group.

Activated immune cells produce TNF-α and also other pro-inflammatory cytokines in chronic renal disorders, which stimulate the release of chemo-attractive molecules by tubular epithelial cells(36). It also recruits leukocytes to tubulointerstitium, increasing inflammation, tubulointerstitial damage, and renal dysfunction. Similarly, the results of our study showed that infiltrated immune cells increased parallel with expression in TNF-α mRNAs in 30 and 700 mg/kg groups. In 30 mg/kg group tubulointerstitial damage, unlike 700 mg/kg group, was found. It seems that the upregulation of TNF-α in 700 mg/kg group was because of increased infiltrated leukocytes that are the early stage of renal injury. This inflammatory response is because of the oxidative stress caused by AgNPs and results in vascular congestion.

The positive association between TGF-β1 expression and the severity of the tubulointerstitial injury and renal dysfunction has been reported in studies in which upregulation of TGF-β1 is correlated with increased risk of progression from chronic renal disease to end-stage renal failure(12, 37).

It has shown that TGF-β1 contributes to tubulointerstitial damage and renal dysfunction through the loss of tubular epithelial cells, by inducing apoptosis, increasing fibrosis. Similarly, our results showed more prominent histological changes in 30, 125, and then 300 mg/kg groups.

Our finding revealed an increase in TGF-β1, TNF-α and, EGF mRNA in some treated groups compared to controls but failed to show any statistically significant correlation between them and caspase-3 or TUNEL+ cells.

A study by Gobe et al. exhibited that the expression of EGF and Bcl-2 in distal tubules increases in the ischemic kidney, leading to distal tubule stress resistance(38). On the other hand, according to the significant increase of Bcl-2 in the 300 mg/kg group compared to the other groups, the decreased expression of EGF seems to have led to an increase in apoptosis.

Conclusion

The present study demonstrated that the AgNPs were induced renal toxicity at both morphological and transcription levels by repeated oral administration. We conclude that renal fibrosis is associated with progressive tubular and glomerular changes in experimental groups. Furthermore, the ratio of Bax / Bcl-2 mRNA was correlated with caspase-3 positive cells. The findings indicate a possible implication of Bax and Bcl-2 in the apoptotic process during AgNPs treatment. The transcription levels of TGF-β1, TNF-α, and EGF have correlated to Bax, and Bcl-2 mRNA expression provides evidence that these growth factors might be involved in the apoptosis regulation.

Abbreviations

AgNPs: Silver nanoparticles, PAS: periodic acid-Schiff, TUNEL: terminal deoxynucleotidyl transferase dUTP nick end labelling, RT-PCR: real-time PCR, EGF: Epidermal Growth Factor, TNF-α: Tumour Necrosis Factor α, TGF-β1: transforming growth factor β1, DLS: dynamic light scattering, H&E: hematoxylin and eosin, BUN: blood urea nitrogen, Ct: Cycle threshold

Declarations

Ethics approval and consent to participate

The above-mentioned treatment/sampling protocols were approved by the ethics committee of Hamadan University of Medical Sciences (ethical code: IR.UMSHA.REC.1394.553) and all methods were carried out in accordance with the relevant guidelines and regulations. The study was carried out in compliance with the ARRIVE guidelines.

Consent for publication

Not applicable

Availability of data and materials

All data generated or analysed during this study are included in this published article.

Competing interests

The authors declare that they have no competing interests.

Funding

This study was funded by Vice-chancellor for Research and Technology, Hamadan University of Medical Sciences, Hamadan Iran (No. 9311145896).

Authors' contributions

HN, MH, MS, MA, NS performed the histological and molecular examinations of the kidney and were contributors in writing the manuscript. ZG treated the animals. ZA designed the study and was a major contributor in writing the paper. All authors read and approved the final manuscript

Acknowledgements

Not applicable

References

1. Zhang X-F, Liu Z-G, Shen W, Gurunathan S. Silver Nanoparticles: Synthesis, Characterization, Properties, Applications, and Therapeutic Approaches. International Journal of Molecular Sciences.17(9):1534.
2. Vance ME, Kuiken T, Vejerano EP, McGinnis SP, Hochella Jr MF, Rejeski D, et al. Nanotechnology in the real world: Redeveloping the nanomaterial consumer products inventory. Beilstein journal of nanotechnology.6(1):1769-80.
3. Bergin IL, Witzmann FA. Nanoparticle toxicity by the gastrointestinal route: evidence and knowledge gaps. International journal of biomedical nanoscience and nanotechnology.3(1-2):163-210.
4. Ji JH, Jung JH, Kim SS, Yoon J-U, Park JD, Choi BS, et al. Twenty-eight-day inhalation toxicity study of silver nanoparticles in Sprague-Dawley rats. Inhalation toxicology. 2007;19(10):857-71.
5. Crosera M, Bovenzi M, Maina G, Adami G, Zanette C, Florio C, et al. Nanoparticle dermal absorption and toxicity: a review of the literature. International archives of occupational and environmental health. 2009;82(9):1043-55.
6. Kim YS, Kim JS, Cho HS, Rha DS, Kim JM, Park JD, et al. Twenty-eight-day oral toxicity, genotoxicity, and gender-related tissue distribution of silver nanoparticles in Sprague-Dawley rats. Inhalation toxicology. 2008;20(6):575-83.
7. Sambale F, Wagner S, Stahl F, Khaydarov RR, Scheper T, Bahnemann D. Investigations of the toxic effect of silver nanoparticles on mammalian cell lines. Journal of Nanomaterials.16(1):6.
8. Mahmoudian ZG, Sohrabi M, Lahoutian H, Assari MJ, Alizadeh Z. Histological alterations and apoptosis in rat liver following silver nanoparticle intraorally administration. Entomology and Applied

Science Letters.3(5):27-35.
9. Xu L, Li X, Takemura T, Hanagata N, Wu G, Chou LL. Genotoxicity and molecular response of silver nanoparticle (NP)-based hydrogel. Journal of nanobiotechnology.10(1):16.
10. Mooney A, Jobson T, Bacon R, Kitamura M, Savill J. Cytokines promote glomerular mesangial cell survival in vitro by stimulus-dependent inhibition of apoptosis. The Journal of Immunology. 1997;159(8):3949-60.
11. Ortiz A, Lorz C, Catalán MP, Danoff TM, Yamasaki Y, Egido J, et al. Expression of apoptosis regulatory proteins in tubular epithelium stressed in culture or following acute renal failure. Kidney international. 2000;57(3):969-81.
12. Teteris SA, Menahem S, Perry G, Maguire JA, Dowling J, Langham RG, et al. Dysregulated growth factor gene expression is associated with tubulointerstitial apoptosis and renal dysfunction. Kidney international. 2007;71(10):1044-53.
13. Ding G, Reddy K, Kapasi AA, Franki N, Gibbons N, Kasinath BS, et al. Angiotensin II induces apoptosis in rat glomerular epithelial cells. American Journal of physiology-renal physiology. 2002;283(1):F173-F80.
14. Pourhamzeh M, Mahmoudian ZG, Saidijam M, Asari MJ, Alizadeh Z. The Effect of Silver Nanoparticles on the Biochemical Parameters of Liver Function in Serum, and the Expression of Caspase-3 in the Liver Tissues of Male Rats. Avicenna Journal of Medical Biochemistry.4(2).
15. Livak KJ, Schmittgen TD. Analysis of relative gene expression data using real-time quantitative PCR and the 2− ΔΔCT method. methods. 2001;25(4):402-8.
16. McAuliffe ME, Perry MJJN. Are nanoparticles potential male reproductive toxicants? A literature review. 2007;1(3):204-10.
17. Kim W-Y, Kim J, Park JD, Ryu HY, Yu IJJJoT, Environmental Health PA. Histological study of gender differences in accumulation of silver nanoparticles in kidneys of Fischer 344 rats. 2009;72(21-22):1279-84.
18. Pronk M, Wijnhoven SW, Bleeker E, Heugens EH, Peijnenburg WJ, Luttik R, et al. Nanomaterials under REACH. Nanosilver as a case study. 2009.
19. Yang L, Kuang H, Zhang W, Aguilar ZP, Wei H, Xu H. Comparisons of the biodistribution and toxicological examinations after repeated intravenous administration of silver and gold nanoparticles in mice. Scientific reports. 2017;7(1):3303.
20. Zuckerman JE, Gale A, Wu P, Ma R, Davis ME. siRNA delivery to the glomerular mesangium using polycationic cyclodextrin nanoparticles containing siRNA. Nucleic acid therapeutics. 2015;25(2):53-64.
21. Day W, Hunt J, McGiven A. Silver deposition in mouse glomeruli. Pathology. 1976;8(3):201-4.
22. Park E-J, Bae E, Yi J, Kim Y, Choi K, Lee SH, et al. Repeated-dose toxicity and inflammatory responses in mice by oral administration of silver nanoparticles. Environmental toxicology and pharmacology. 2010;30(2):162-8.

23. Scott K, Webb M, Sorrentino SA. Long-Term Caring-e-Book: Residential, home and community aged care: Elsevier Health Sciences; 2015.
24. Awadalla EA, Salah-Eldin A-E. Histopathological and molecular studies on tramadol mediated hepato-renal toxicity in rats. J Pharm Biol Sci. 2015;10(6):90-102.
25. Ibrahim K, Al-Mutary M, Bakhiet A, Khan H. Histopathology of the liver, kidney, and spleen of mice exposed to gold nanoparticles. Molecules. 2018;23(8):1848.
26. Ma P, Luo Q, Chen J, Gan Y, Du J, Ding S, et al. Intraperitoneal injection of magnetic Fe3O4-nanoparticle induces hepatic and renal tissue injury via oxidative stress in mice. International journal of nanomedicine. 2012;7:4809.
27. Abdelhalim MAK, Jarrar BM. Renal tissue alterations were size-dependent with smaller ones induced more effects and related with time exposure of gold nanoparticles. Lipids in Health and Disease. 2011;10(1):163.
28. Sahu BD, Kuncha M, Sindhura GJ, Sistla R. Hesperidin attenuates cisplatin-induced acute renal injury by decreasing oxidative stress, inflammation and DNA damage. Phytomedicine. 2013;20(5):453-60.
29. Curthoys NP, Moe OW. Proximal tubule function and response to acidosis. Clinical Journal of the American Society of Nephrology. 2014;9(9):1627-38.
30. Abuelo JG. Normotensive ischemic acute renal failure. New England Journal of Medicine. 2007;357(8):797-805.
31. Sadek EM, Salama NM, Ismail DI, Elshafei AA. Histological study on the protective effect of endogenous stem-cell mobilization in Adriamycin-induced chronic nephropathy in rats. Journal of microscopy and ultrastructure. 2016;4(3):133-42.
32. Bedi S, Vidyasagar A, Djamali A. Epithelial-to-mesenchymal transition and chronic allograft tubulointerstitial fibrosis. Transplantation Reviews. 2008;22(1):1-5.
33. Farris AB, Colvin RB. Renal Interstitial fibrosis: mechanisms and evaluation in: current opinion in nephrology and hypertension. Current opinion in nephrology and hypertension. 2012;21(3):289.
34. Havasi A, Borkan SC. Apoptosis and acute kidney injury. Kidney international. 2011;80(1):29-40.
35. Yang B, Johnson TS, Thomas GL, Watson PF, Wagner B, Skill NJ, et al. Expression of apoptosis-related genes and proteins in experimental chronic renal scarring. Journal of the American Society of Nephrology. 2001;12(2):275-88.
36. Kuroiwa T, Schlimgen R, Illei GG, McInnes IB, Boumpas DT. Distinct T cell/renal tubular epithelial cell interactions define differential chemokine production: implications for tubulointerstitial injury in chronic glomerulonephritides. The Journal of Immunology. 2000;164(6):3323-9.
37. August P, Suthanthiran M. Transforming growth factor beta and progression of renal disease: Management of comorbidities in kidney disease in the 21st century: Anemia and bone disease. Kidney international. 2003;64:S99-S104.
38. Gobe G, Zhang X-J, Willgoss DA, Schoch E, Hogg NA, Endre ZHJJotASoN. Relationship between expression of Bcl-2 genes and growth factors in ischemic acute renal failure in the rat.

2000;11(3):454-67.

Figures

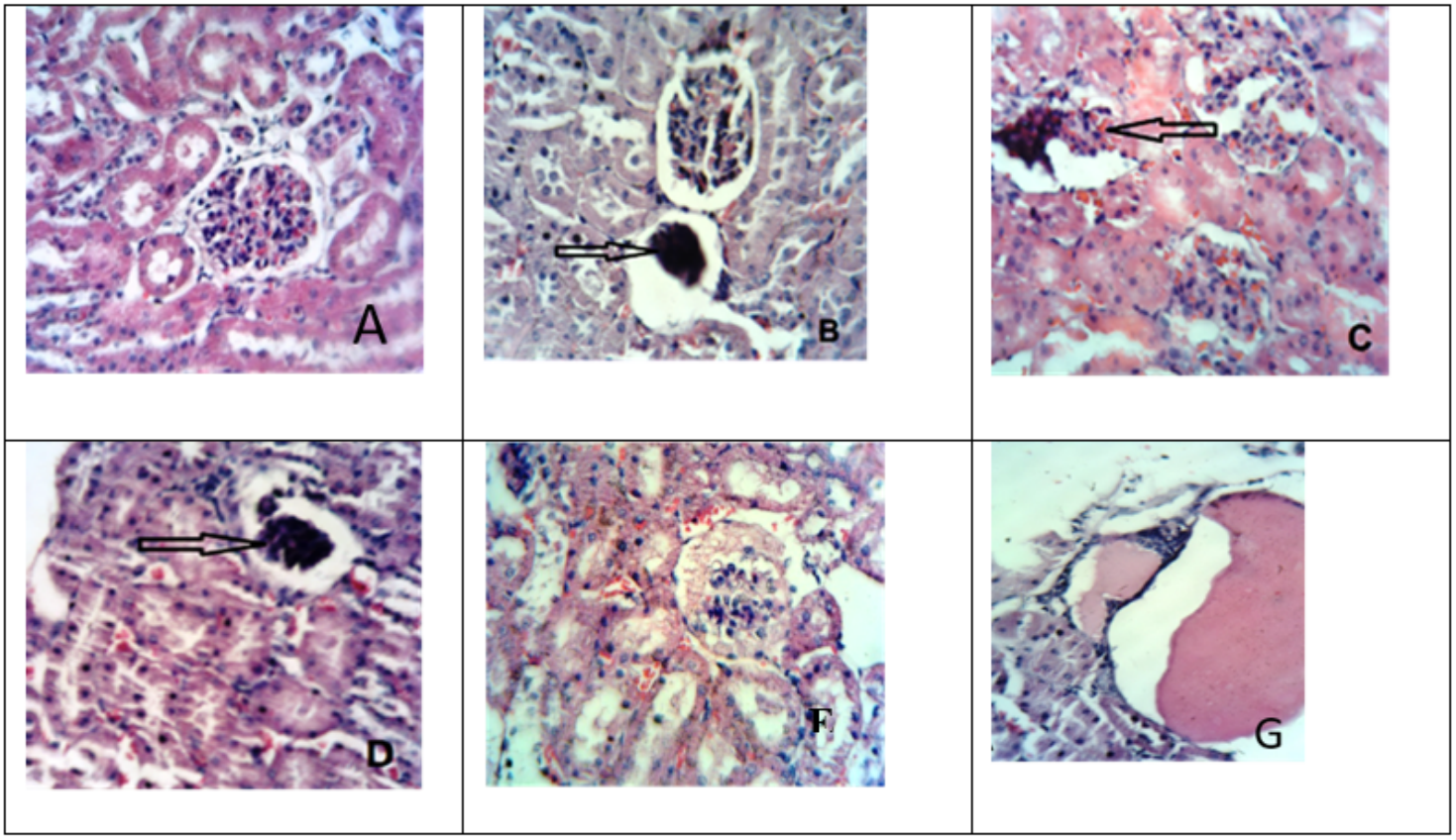

Figure 1

Light photomicrograph of rat kidney tissues [H&E stain × 400]: control group (A) the renal cortex shows normal architecture. AgNPs treated groups (B) 30mg/kg, (C) 125 mg/kg, (D) 300g/kg showing marked degenerative changes in the glomeruli appeared necrotic with loss of glomerular tufts and wide Bowman's space (arrow), (E) 700 mg/kg shows swelled renal glomerulus. Example of hyaline casts in renal tubul in125mg/kg treated group. Congestion of the capillary loops, infiltration of inflammatory cells and disorganization of tubules are see in teated groups. Table shows effect of various concentrations of silver nanoparticles on diameter of glomeruli. There were significant differences between treated groups and relation to control. a: compared to control group (P=0.001), b: compared to 30mg/kg group (P=0.001), c: compared to 125mg/kg group (P=0.001), d:compared to 300mg/kg group (P=0.001), e: compared to 700 mg/kg group(P=0.001).

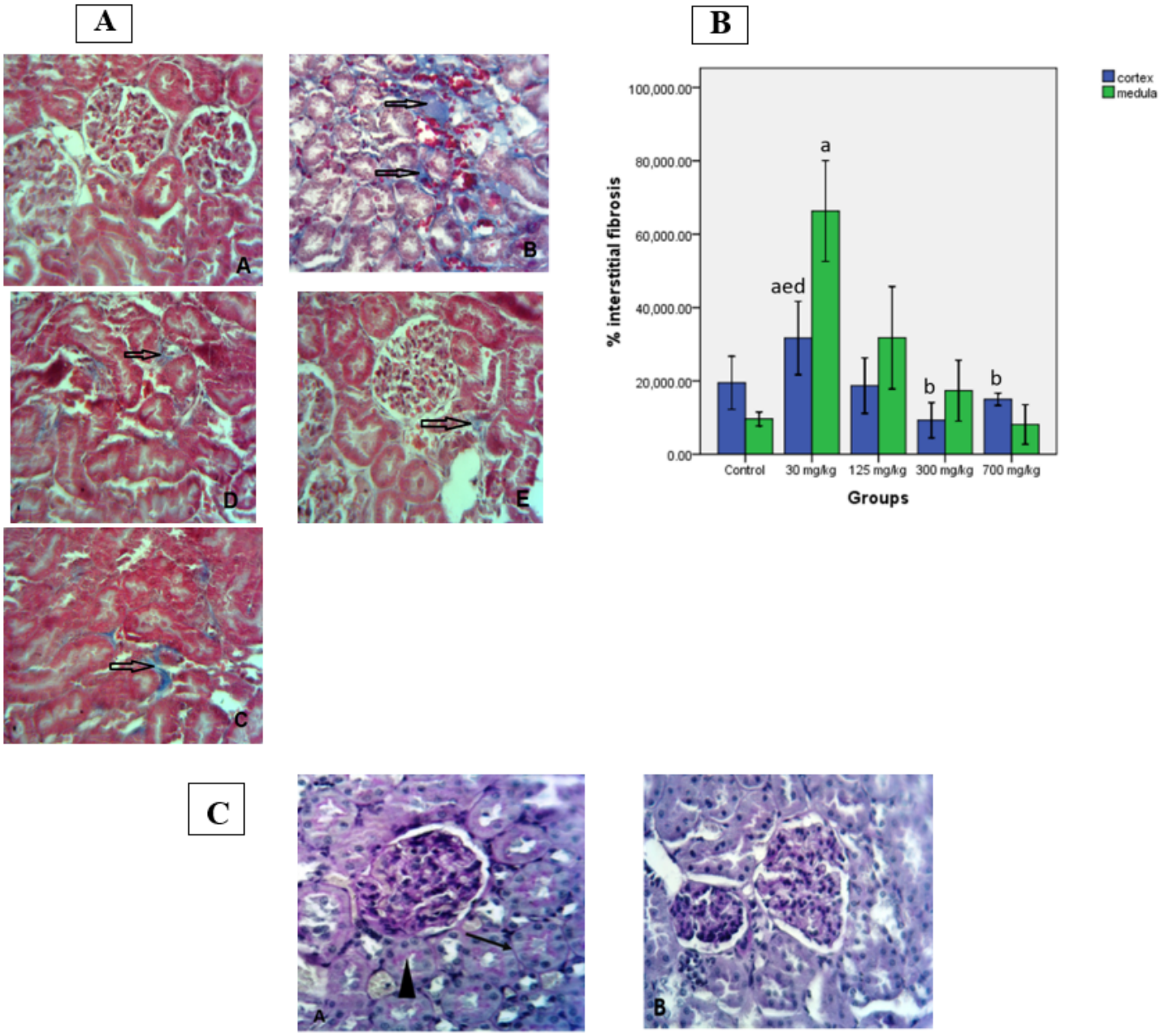

Figure 2

Kidney sections were stained with Masson trichrome (A and B) and periodic acid Schiff (PAS) (C). B: collagen depositions were quantified as the number of pixels of blue color of the medulla and cortex of the kidney using image J analysis software. There were significant differences (P<0.05) between treated groups and relation to control group that has shown with a: compared to control group (P<0.05), b: compared to 30mg/kg group, c: compared to 125mg/kg group, d: compared to 300mg/kg group, e: compared to 700 mg/kg group. C: Renal cortex of in control group (A) shows cortical tubules with intact brush border (triangle) and clear basal lamina (arrowheads). (B) Section from 30 mg/kg shows partial or complete loss of brush border in some of the tubules, the tubular basal laminae are interrupted at many sites.

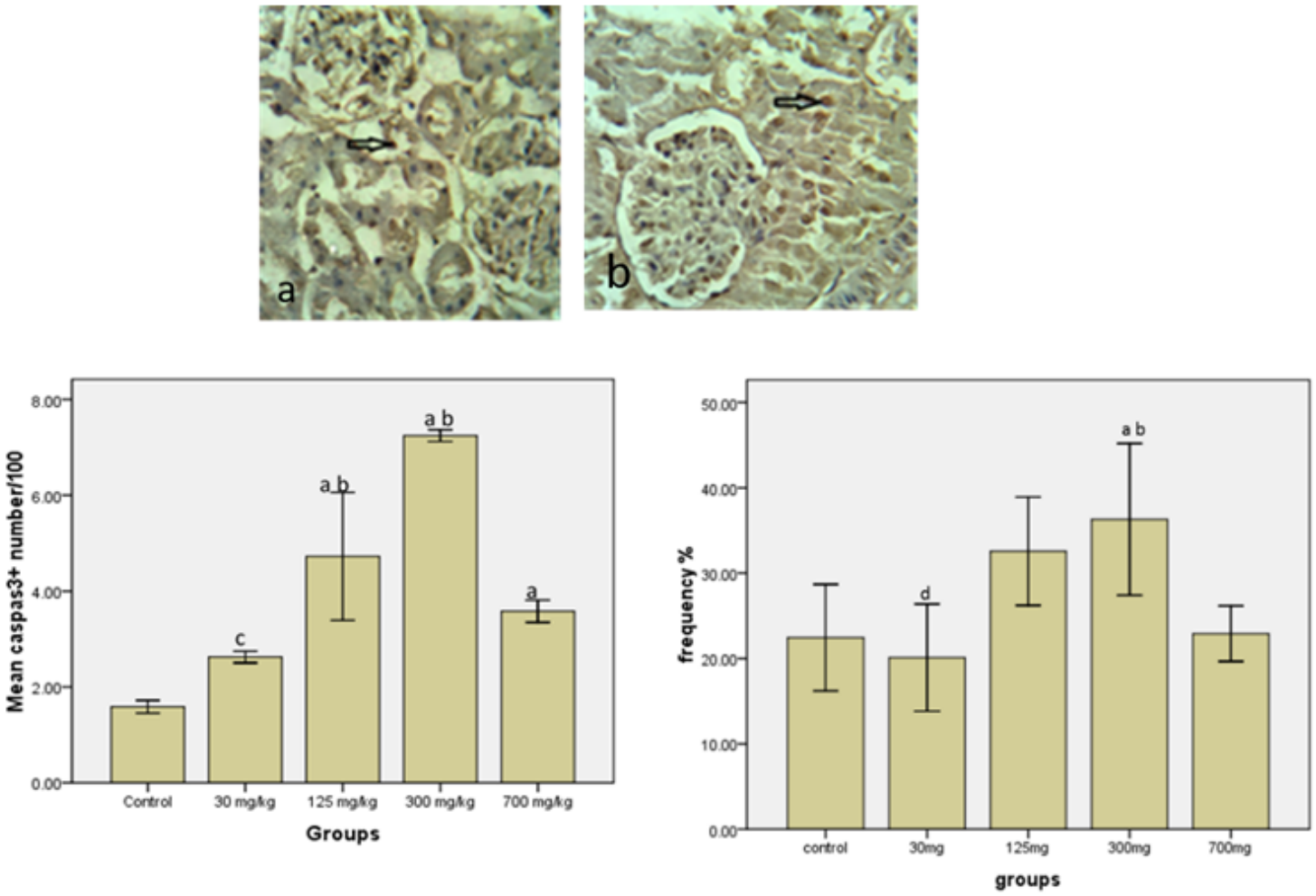

Figure 3

Cell apoptosis detected by TUNEL and Caspase-3 immunostaining in the renal tubule epithelial cell, 28 days post-exposure different doses of AgNPs. There were significant differences ($P<0.05$) between treated groups and relation to control group that has shown with a, b, c, d and e. a: compared to control group ($P=0.001$), b: compared to 30mg/kg group, c: compared to 125mg/kg group, d: compared to 300mg/kg group, e: compared to 700 mg/kg group. Examples of TUNEL-positive the tubule epithelial cell in 125 (a) and 300 (b) mg/kg AgNPs treated group(X400).

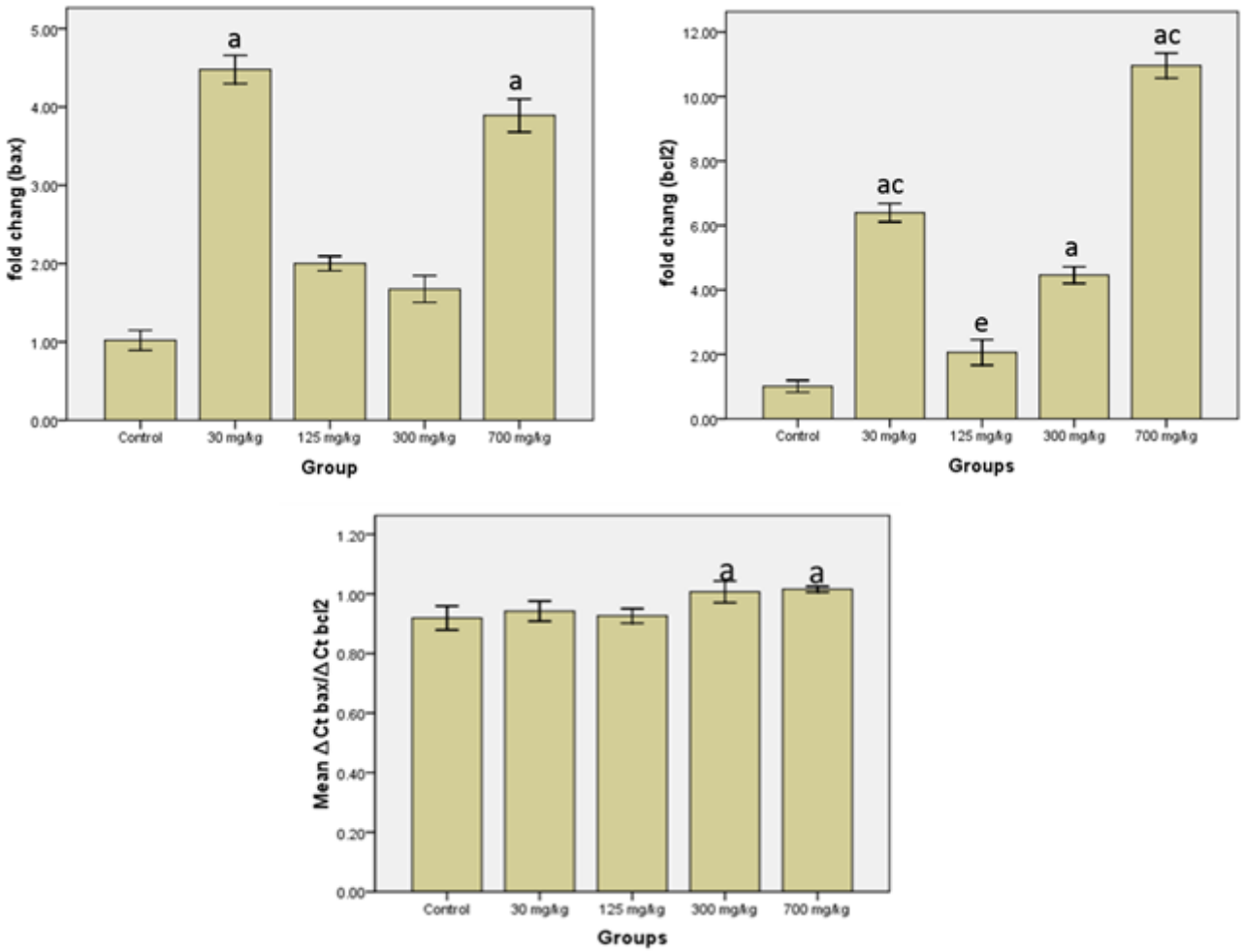

Figure 4

Bax and Bcl-2 genes expression and the ratio of Bax to Bcl-2 changes in the kidney of rats treated with AgNPs. There were significant differences (P<0.05) between treated groups and relation to control that has shown with a, c, and e. a: compared to control group, c: compared to 125mg/kg group, e: compared to 700 mg/kg group

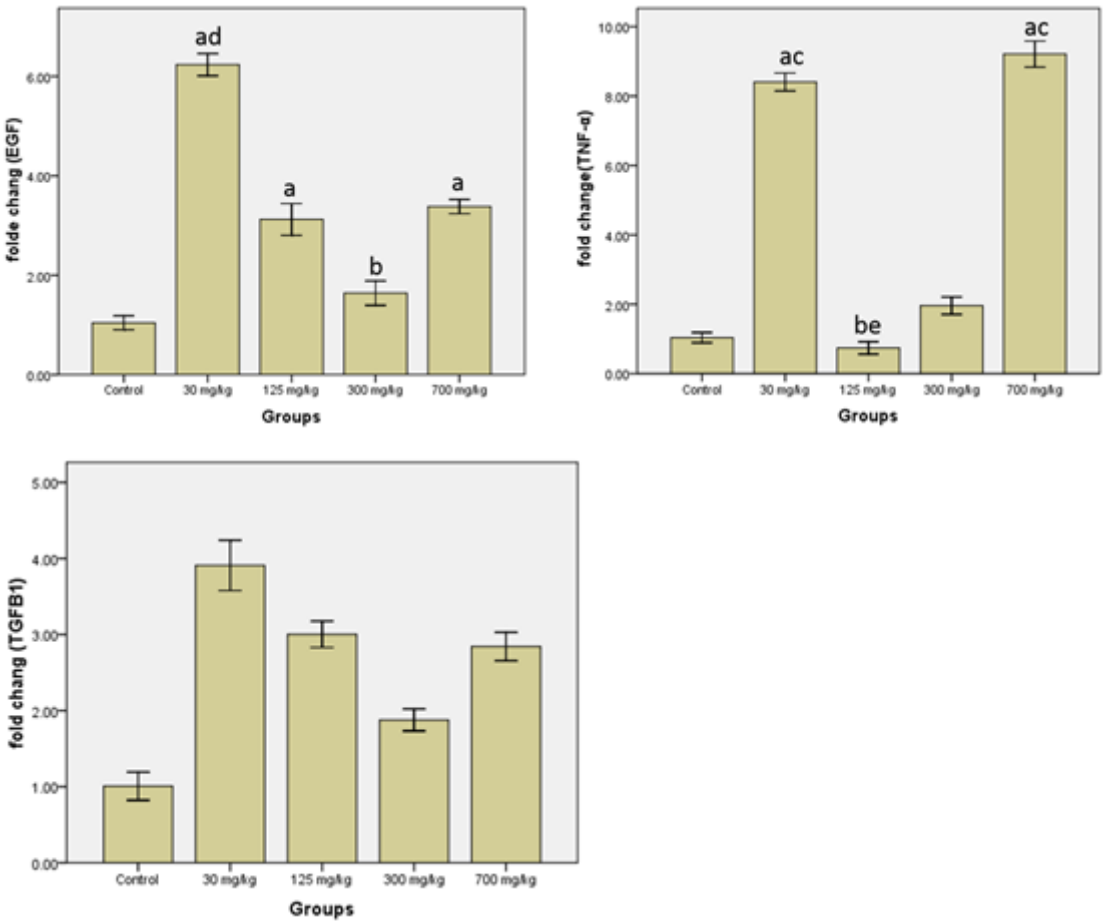

Figure 5

Growth factor gene expression is altered in AgNPs treated groups. There were significant differences (P<0.05) between treated groups and relation to control that has shown with a, b, c, d and e. a: compared to control group, b: compared to 30mg/kg group, c: compared to 125mg/kg group, d: compared to 300mg/kg group, e: compared to 700 mg/kg group.